A secondary metabolites produced by Streptomyces ssp. XY-R31 suppresses LPS-induced inflammatory responses through NF-κB, MAPKs, and HO-1 Pathways in RAW264.7 cells

Ying Xu (✉ boxuying@szu.edu.cn)
Shenzhen University

Yang-yang Yu
Shenzhen University Health Science Center

Si-man Zheng
Shenzhen University

Ran Fang
Shenzhen University Health Science Center

Research Article

Abstract

Inflammation response is a complex physiological process and suppression of inflammation activated in macrophages induced by LPS is an important target for treatment of various chronic diseases. A crude extract produced by *Streptomyces* ssp. (R31 crude extract) which was isolated from a mangrove sediment showed a significant inhibitory effect in LPS-stimulated inflammatory response. In this study, R31 crude extract decreased the NO production dose-dependently. The release of IL-6 and IL-10 in macrophages were reduced upon pretreatment of R31 crude extract. In addition, R31 crude extract treatment inhibited the translocation of NF-κB and NFAT into the nucleus and the phosphorylation of MAPKs as well as AKT. On the other hand, R31 crude extract induced HO-1 expression in LPS-stimulated macrophage. Collectively, these findings indicate that R31 crude extract exhibited an anti-inflammatory effect and is a potential therapeutic candidate for the treatment of inflammatory diseases.

1. Introduction

Inflammation is a normal immunological defense reaction that generally occurs in response to invading foreign pathogens and various internal or external harmful stimuli which induce systemic injuries[1]. This process is usually accompanied by the release of the various inflammatory mediators by various immune cells[2]. However, excessive inflammatory response and increased production of inflammatory mediators are reported to result in the development of many disease complications such as neurological diabetes, hepatitis, rheumatoid arthritis, atherosclerosis and asthma. Hence, suppression of over-inflammatory is thought to be an important treatment to control the development of disease complications. Macrophages are the major inflammatory cells which initiate and modulate the host inflammatory response[3]. Within the overwhelming studies on inflammation, the most commonly used in vitro model to investigate anti-inflammatory activity from natural compounds is RAW264.7 (a monocyte/macrophage-like cell line) induced by Lipopolysaccharide (LPS)[4].

LPS, an essential component of the outer membrane of Gram-negative bacteria, is one of the common stimuli in macrophages inflammatory actives. LPS signaling is initiated by binding with the LPS-binding protein (LBP), CD14, the lipid-binding accessory protein MD-2, and the Toll-like receptor 4 (TLR4) protein complex. Following the increase of reactive oxygen species (ROS), it activates the downstream signaling pathways of NF-κB, MAPKs, Janus kinase-signal transducers and activators of transcription (JAK-STATs) to trigger the release of numbers of inflammatory mediators such as iNOS, COX-2, monocyte chemoattractant protein-1 (MCP-1), IL-6, TNF-α and so on[5].

The HO-1 gene has been reported to be an important Nrf2-regulated antioxidant enzyme that controls intracellular reactive oxygen species (ROS) levels from varied stimuli. A study has suggested that knockout of HO-1 in mice resulted in hypersensitive response to pro-inflammatory stimuli through increasing the expression of inflammatory mediator, including IL-6 and TNF-α[6]. Another study suggested that up-regulation of the NRF2/HO-1 expression suppressed the TLR4/NF-B-mediated pro-inflammatory mediators[7]. Furthermore, previous studies indicated that there is a pertinence between the HO-1

signaling pathway and the NF-κB signaling pathway, and the production of pro-inflammatory cytokines by HO-1 activation inhibited the NF-κB signaling pathway[8]. These results suggest that modulation of HO-1-Nrf2 signaling pathway in the inflammatory cells would be an appropriate access to control inflammatory reactions.

It is well known that marine organisms are an important source of natural products[9]. These naturally occurring secondary metabolites have proved to be a rich and potential candidate to the treatment of cancer, inflammation disease and etc. Mangroves occur at the interface between terrestrial and marine habitats and have their roots inundated with seawater. The uniqueness of the mangrove environment, including high salinity, low oxygen, nutrient limitation, tidal gradients, high temperatures, excessively high light, and drought, may prompt the microbes which inhabited in mangrove to generate diverse functional metabolites. As reported, bacteria and fungi constitute 91% of the total microbial biomass. Actinomycetes have been used for drug discovery for more than five decades, and marine actinomycetes have been reported to be an excellent source for their potential to produce bioactive natural products with novel structures[10]. Of these, about 75% are derived from Streptomycetes[11]. Recently, we isolated a strain of *Streptomyces* ssp. from a sample of mangrove sediment, Mai Po, Hongkong, China. In this study, we focused on the anti-inflammatory effect of the secondary metabolites produced by *Streptomyces* ssp. (*R31 crude extract*) in LPS-stimulated RAW 264.7 cells.

2. Materials And Methods

2.1 materials

The cell culture medium DMEM, fetal bovine serum (FBS), Penicillin-Streptomycin and 0.25% trypsin-EDTA were purchased from Gibco (Thermo Fisher Scientific, Inc., Waltham, MA, USA). LPS-EK Ultrapure was purchased from invivogen. Antibodies directed against HO-1 (ab85309), COX-2 (ab62331), as well as HRP-conjugated secondary antibodies (ab6721) were purchased from abcam. Lamin B1 (12987-1-AP), α-tubulin (14555-1-AP), were purchased from ProteinTech. Antibodies directed against iNOS (13120S), protein kinase B (Akt; 4685S), p-Akt (4060S), NF-κB (8242S), NFAT1 (4389S), β-actin (4967S), and MAPKs [P38, 8690S; phospho-P38, 4511S; JNK, 9252S; phospho-JNK, 4668S; ERK, 4695S; phospho-ERK, 4370S], were purchased from Cell Signaling Technology, Inc., (Danvers, MA, United States).

2.2 strain identification

The strain of actinomycete was isolated from the sediment samples of Mai Po mangroves, Hongkong, China and grown on R2A agar (#218263, BD difco). This strain was identified as *Streptomyces* ssp. based on phylogenetic analysis of 16S rRNA gene sequence using primers 8F (5-AGAGTTTGATCCTGGCTCA-3) and 1942R (5-GGTTACCTTGTTACGACTT-3).

2.3 strain fermentation and extraction

This *Streptomyces* was activate on R2A agar first, then inoculated and cultured in 50 mL Centrifuge tube containing 15 mL culture medium (starch 5.0 g, glucose 5.0 g, tryptone 1.0 g, yeast extract 1.0 g, peptone 1.0 g, seasalt 17.0 g in 1L Deionized water, ph 7.0), incubated on a rotary shaker (200 rev/min) at 28°C for 1 days. 4 mL of this seed culture was inoculated into 250 mL Erlenmeyer flasks containing 80 mL culture medium, incubated at 28°C with shaking (200 rpm) for 4 days. The cell culture medium was centrifuged at 10,000× g for 15 min to remove precipitates and use filter paper to separate the mycelia. The supernatant was mixed with triple volume of ethyl acetate and then the aqueous and ethyl acetate phases was separated. The ethyl acetate layer was evaporated under a rotary evaporator (Heidoloph) to obtain crude extract R31 crude extract which was redissolved in DMSO.

2.4 cell culture

The murine macrophage cell line RAW264.7 was purchased from American Type Culture Collection (Manassas, VA, USA). Cells were cultured in DMEM supplemented with 10% heat-inactivated foetal bovine serum (FBS), and 1% penicillin-streptomycin at 37°C in a 5% CO_2 humidified atmosphere.

2.5 cytotoxicity assay

The cell viability was measured by using the Cell counting kit-8 assay (DOJINDO). Briefly, RAW24.7 cells were seeded into 24-well plates at a density of 5×10^5 cells per well for 24 h and treated with various concentrations of R31 crude extract (5, 10, 15, 20, 25 µg/ml) or co-treated with LPS (1 µg/ml) for another 24 h at 37°C. Thereafter, we replaced the supernatants for new medium and CCK-8 solution (100 µl/ml) was added to each well, the cells were cultured for another 30 min at 37°C. Finally, the 24-well plates was measured at 450nm absorbance by a microplate reader (Benchmark plus Bio-Rad Laboratories, CA, USA).

2.6 measurement of nitrite concentration

To measure nitrite, the cells were pretreated with R31 crude extract followed by LPS stimulation as described above. Cells were treated with or without R31 crude extract in the presence or absence of LPS for 24 h. 100-µl cell-free supernatants were collected and mixing with the Griess reagent which containing equal volumes of 1% sulfanilamide in 2.5% H3PO4 with 0.1% N-(1-naphthyl)- ethylenediamine dihydrochloride. Each sample was assayed in duplicate. Nitrite content was measured by absorbance at 540nm with a microplate reader (Benchmark plus Bio-Rad Laboratories, CA, USA).

2.7 RNA-sequencing and function enrichment analysis

The samples of control, R31 crude extract (25 µg/ml) group both with or without LPS (1 µg/ml) were sent to Beijing Genomics Institute (BGI, Shenzhen, China) for RNA extraction, cDNA library construction and sequencing on DNBSEQ platform, generating an average of 45.57 M reads of 150 bp per sample. Adapter and low quanlity reads (N > 5%, Q < 10) were removed by SOAPnuke v1.5.2. Differentially expressed genes (DEGs) between the sample groups were screened out from normalized TPM values, |log2 (fold change)| ≥1 and P-value ≤ 0.05. VENN diagram is constructed by Dr.TOM (BGI) system to show the numbers of DEGs between the groups, then the Heat Maps, Gene Ontology (GO) and Kyoto Encyclopedia of Genes and Genomes (KEGG) analysis were performed base on these DEGs.

2.8 quantitative realtimepolymerase chain reaction (qRTPCR)

RAW264.7 cells were seeded into a 6-well plates overnight and treated with R31 crude extract (25 µg/ml) and LPS for 4 h at 37°C. Total cellular RNA was isolated using AxyPrep™ Multisource Total RNA Miniprep Kit (Axygen, Corning Inc., NY, USA) according to the manufacturer's instructions. RNA concentrations were determined by NanoDrop ND1000. From each sample group, total RNA (1 µg) was reverse-transcribed to obtain cDNA using PrimeScript™ RT reagent Kit with gDNA Eraser (RR047A, Takara, Japan). Real-time PCR was performed by using QuantStudio 3 Real-Time PCR Systems (Applied Biosystems) and TB Green® Premix Ex Taq™ II (RR820A, Takara, Japan). Relative fold change of target mRNA were determined using the comparative cycle threshold ($\Delta\Delta CT$) method by normalizing target mRNA Ct values to those for β-actin (Ct). The qRT-PCR reaction conditions were as follows: 95°C for 30 s, followed by 40 cycles of 95°C for 5 s, 60°C for 30 s. In addition, a melting curve analysis was carried out to verify non-specific signals. Each sample was performed in triplicate. Primer sequences for qPCR of iNOS, COX-2, HO-1 and β-actin mRNA are shown in Table 1.

Table 1
Name and sequence of primers used for reverse transcription-quantitative polymerase chain reaction.

Gene name	Primer sequence (5'-3')	Gene ID	Product size (bp)
Inducible nitric oxide synthase	F: GGCACCGAGATTGGAGTTC R: GGTCACATTCTGCTTCT	NM001313921	174
Cyclooxygenase-2	F: TCAGGTCATTGGTGGAGAGG R: ATGGTGGCATACATCATCAGAC	NM011198.4	150
Heme oxygenase-1	F: AGGTCCTGAAGAAGATTGC R: TCTCCAGAGTGTTCATTCG	NM010442.2	175
β-actin	F: GCACCACACCTTCTACAA R TACGACCAGAGGCATACA	NM007393.5	156
F, forward; R, reverse.			

2.9 measurement of IL-1, IL-6, IL-10 and TNF-α concentration

To detect the cytokine production, the cells were pretreated with different concentrations of R31 crude extract (5–25 µg/ml) for 30 min (37˚C) and stimulated by LPS (1 µg/ml) for 24 h at 37˚C. The levels of IL-1, IL-6, IL-10 and TNF-α in the culture media was measured by an enzyme-linked immunosorbent assay (ELISA) kit (Invitrogen, Thermo Fisher Scientific, Inc., Waltham, MA, USA) according to the manufacturer's instructions.

2.10 preparation of nuclear extract

The RAW264.7 cells were treated with R31 crude extract (25 µg/ml) followed by stimulated with LPS for 30 min at 37˚C. The cells were washed three times with cold PBS and use the extraction of cytoplasmic and nuclear protein with the kit (#P0027, Beyond time, Shanghai, China) to obtain the cytoplasmic and nuclear proteins and then stored at -80∘C.

2.11 western blot analysis

RAW264.7 cells were seeded into a 6-well plates overnight and treated with R31 crude extract (25 µg/ml) and LPS for 15 min at 37˚C. Then the cells were harvested by using an ice-cold RIPA buffer (Beyotime) containing protease and phosphatase inhibitor (#539134, #524629, Millipore, Billerica, MA, USA). Protein concentrations of the cell lysates were determined by using the BCA protein assay reagent (Beyotime) according to the manufacturer's instructions. Total proteins of each sample (20 µg) were separated by 10% SDS-PAGE gels and transferred to PVDF membrane (#IPVH00010, Merck Millipore). After blocking with 5% non-fat milk in Tris-buffered saline (TBS) containing 0.1% Tween-20 (TBST) at room temperature for 1 h, the membranes were incubated with primary antibodies directed against p-p38, p38 (1:1,000), p-ERK, ERK (1:1,000), p-JNK, JNK (1:1,000), p-Akt, Akt (1:1,000), HO-1 (1:1,000), iNOS (1:1000), COX-2 (1:1,000), NFAT1 (1:1,000), NF-κB p65 (1:1,000), Lamin B1 (1:1,000), α-tubulin (1:1,000), and β-actin (1:1,000) overnight at 4°C. The PVDF membranes were washed with TBST and incubated with horseradish peroxidase (HRP)- conjugated secondary antibody (1:5000) for 1 h at room temperature. Lamin B1 /α-tubulin/ β-actin was used as the loading control for each lane. After washing with TBST, target signals were visualized by ECL (#32106, Thermo Fisher Scientific) detection and analyzed with a gel imaging software.

2.12 statistical analysis

All experiments were performed at least three times. The data were expressed as the mean ± standard deviation (SD). Statistical analysis was performed using the Statistical Package for GraphPad Prism software (version 16.0) to determine significant differences between the sample groups. We also used either a Student's t-test or one-way analysis of variance followed by Dunnett's multiple comparisons test for analyses. P-values of less than 0.05 was considered to indicate a statistically significant.

3. Results

3.1 R31 crude extract did not exhibit cytotoxicity on macrophage cell

To determined the cytotoxic effect of R31 crude extract on RAW 264.7 macrophage cells, the cells were treated with increasing concentrations (5–25 μg/ml) of R31 crude extract for 24 h and measured by CCK-8. The cells without any treatment were used to be the negative control. As the Fig. 1 shows that R31 crude extract is non-toxic together with or without 1 μg/ml LPS treatment of the cells. Therefore, these concentrations of R31 crude extract were used for further study.

3.2 R31 crude extract inhibited the production of NO release

The cells were pretreated with R31 to determine the regulation of NO release. Compared with the negative control, the cells treated with LPS alone notably increased the production of NO and were significantly and dose-dependently reduced by R31 crude extract treatment (Fig. 2).

3.3 data analysis of DEGs from RNA-Sequence

Differentially expressed genes (DEGs) were screened out under the conditions: |log2 (fold change)|≥1 and P-value ≤ 0.05. As shown in the Venn diagram (Fig. 3A), there are 1808 DEGs identified in control + LPS vs control group while 700 DEGs were identified in R31 crude extract + LPS vs control + LPS group. 373 DEGs responding to control group, LPS-induced and R31 crude extract treatment. A hierarchical cluster analysis (Fig. 3B) represent the expression patterns of the common expressed DEGs in control + LPS vs control group and R31 crude extract + LPS vs control + LPS group, and obviously showed that most up-regulated DEGs due to LPS could be reduced by R31 crude extract, and vice versa. As shown in Fig. 4A, the differentially expressed genes were significantly enriched in various biological process by GO database, including the cellular response to interferon-beta, response to bacterium, immune response, inflammatory response, immune system process, innate immune response, regulation of signaling receptor activity. Also the target genes were mapped to KEGG database, the top 10 KEGG pathways significantly enriched in inflammatory responses (Fig. 4B), including TNF signaling pathway, Cytokine-cytokine receptor interaction, NOD-like receptor signaling pathway, IL-17 signaling pathway, Cellular senescence, NF-kappa B signaling pathway, Jak-STAT signaling pathway, Chemokine signaling pathway, Toll-like receptor signaling pathway.

3.4 R31 crude extract inhibits the expression of inflammatory cytokines in LPS-stimulated macrophage cells

Activation of COX-2 and iNOS are both pivotal inflammatory indicators in inflammatory-related diseases. In our study, we performed qRT-PCR to verify whether the reduced levels of NO was due to decreased COX-2 or iNOS expression. Compared to the non-treated group (Fig. 5A, B), LPS treatment alone increased the

COX-2 and iNOS mRNA expressions, but R31 crude extract didn't show any effects on the COX-2 and iNOS mRNA levels in RAW264.7 macrophage cells.

Treatment with R31 crude extract significantly decreased the release of IL-1 and IL-6 cytokines stimulated by LPS in a dose-dependent manner from RAW264.7 cells (Fig. 6A, B). However, R31 crude extract did not influence the secretion of TNF-α treated by LPS (Fig. 6C). These results showed that R31 crude extract inhibited inflammatory responses in LPS-stimulated RAW264.7 cells by suppressed the production of pro-inflammatory cytokines.

3.5 R31 crude extract promoted the activation of HO-1 pathway

HO-1 activation has been considered to be a major anti-inflammatory modulator in macrophage. To determine the modulatory effect of association of R31 crude extract on HO-1 activation, we investigate the HO-1 mRNA levels by RT-qPCR. As shown in Fig. 7, cells pretread with R31 crude extract significantly increased HO-1 mRNA levels.

3.6 R31 crude extract inhibited LPS-stimulated NF-κB and NFAT nuclear translocation.

Studies have demonstrated that eukaryotic transcription factor NF-κB is involved in many inflammatory responses. NF-κB normally presents in the cytosol in an inactive form linked to inhibitor κB (IκB) protein. NF-κ B released from the NF-κB/IκB complex and translocates into the nucleus when IκB protein degraded to response to an activation signal. Therefore, we measured the nuclear translocation of the NF-κB by Western blot. Treatment with LPS increased the expression of NF-κB in nuclear extracts but was significantly decreased by a pre-treatement of R31 crude extract (Fig. 8A). LPS stimulation would result in NFAT-dephosphorylation by calcineurin. Cytoplasmic NFAT translocates to the nucleus and become transcriptionally active, and induce the activation of number of inflammatory factors. So we also investigated the nuclear translocation of the NFAT induced by LPS, as shown in Fig. 8B, the nuclear translocation of the NFAT induced by LPS was attenuated by pre-treatment with R31 crude extract. In Fig. 8C the fold change of translocation of the NFAT and NF-kB were compared.

3.7 R31 crude extract suppressed LPS-stimulated activation of MAPKs and AKT

It is also known that MAPKs family (p38 MAPK, ERK1/2, JNK) have been delineated to be involved in LPS-stimulated inflammatory responses. Therefore the phosphorylation of MAPKs signaling proteins was evaluated to further determine its potential role in the anti-inflammatory mechanism of R31 crude extract. As shown in the data (Fig. 9A. B. C), exposure of RAW264.7 cell to LPS increased the phosphorylation of p38, ERK1/2, JNK, which were decreased by the treatment of R31 crude extract. Apart from MAPKs, Akt

signaling is crucial for the regulation of inflammatory mediators in activated RAW264.7 cell. LPS-stimulated phosphorylation of Akt was significantly suppressed by R31 crude extract (Fig. 9D).

4. Discussion

In the immunological defense mechanism, macrophages play a vital role in regulating inflammatory responses by producing a variety of inflammatory mediators[12]. However, prolonged activation of macrophages has been demonstrated to contribute to the development of many complications of human disease[13]. For instance, over-release of inflammatory mediators of macrophages in atherosclerotic lesions results in the progression of the lesion into a complicated atherosclerotic plaque[14]. NO and PGE2 are known to be key mediators to induce a number of physiological and pathological processes[15]. Excessive expression of NO and PGE2 are catalyzed by the up-regulation of iNOS and COX-2[16]. Thus, down-regulating the production of these dedicators may inhibit the development of inflammation. In our study, R31 crude extract significantly inhibited the production of NO in a dose-dependent manner.

Cytokines play a crucial roles in the interaction and communication between cells[17]. Macrophages secrete different cytokines to trigger immune response[18]. Cytokines, such as IL-1, IL-6 and TNF-α have been demonstrated to act as pro-inflammatory factors in immune cells[19−20]. Our study showed that R31 crude extract significantly inhibited the expression of IL-1 and IL-6 in a dose-dependent manner. However, R31 crude extract pretreatment did not influence the secretion of TNF-α. These results suggest that R31 crude extract may ameliorate inflammation activated by modulating IL-1 and IL-6 signaling pathways.

NF-κB, which is essential for the expression of iNOS and COX-2, acts as a pivotal role in innate and adaptive immune functions[21]. Previous studies showed that AKT, a serine/threonine kinase has also been implicated in NF-κB activation[22]. In our study, the activation of NF-κB Akt induced by LPS was inhibited by treatment with R31 crude extract. On the other hand, HO-1 acts as a therapeutic molecule in chronic inflammation[23−24]. Studies demonstrated that HO-1 limited NF-κB pathway by inhibiting IκB degradation[25]. We found that the expression of HO-1 mRNA was increased upon R31 crude extract treatment. These results indicate that the inhibition effect of R31 crude extract on LPS stimulation is mediated through the activation of HO-1 signaling and inhibition of Akt-NF-κB-iNOS signaling.

NFAT proteins are phosphorylated and reside in the cytoplasm in resting cells. These gene family consists of 5 members including NFATc1, NFATc2, NFATc3, NFATc4, and NFAT5. When stimulated by diverse signaling pathways, NFAT is dephosphorylated by calcineurin, translocates to the nucleus and becomes transcriptionally active. They transcriptionally regulates numerous cytokines, chemokines, and growth factors to modulate immune responses[26]. In our study, we examined NFAT nuclear−cytoplasmic distribution upon R31 crude extract treatment from LPS-stimulated RAW264.7 macrophages. The results showed that R31 crude extract significantly inhibited NFAT translocation. The result suggests that R31 crude extract could inhibit LPS-induced inflammatory response by inhibiting the dephosphorylation of NFAT.

MAPKs signaling pathway have been demonstrated to be involved in inflammation and immune system by regulating the expression of pro-inflammatory mediators[2]. Previous studies showed that blocking MAPKs by natural compounds influences the inflammatory activity[27]. In the present study, R31 crude extract inhibited the phosphorylation of P38, ERK1/2, JNK without changing their total protein level. The data revealed here showed that R31 crude extract inhibits the LPS-induced inflammatory responses by MAP kinase phosphorylation events.

5. Conclusion

This study demonstrated that R31 crude extract has a significant anti-inflammatory effect on LPS-stimulated inflammatory response from RAW264.7 macrophage cell. R31 crude extract down-regulated the release of pro-inflammatory mediators such as IL-1 and IL-6. In addition, R31 crude extract induced HO-1, reduced translocation of NF-κB and NFAT into the nucleus, and inhibited Akt and MAPKs activation. Our findings provide a possible action of R31 crude extract in inflammatory-related disorders and suggest that R31 crude extract could be a potential therapeutic candidate. Natural small molecules may have novel mechanisms of action. Further study is requied to identify the R31 monomer and reveal its anti-inflammatory molecular mechanism.

Abbreviations

iNOS, inducible nitric oxide synthase; COX-2, cyclooxygenase-2; IL-1, interleukin-1; IL-6, interleukin-6; IL-10, interleukin-10; TNF-α, tumor necrosis factor-α; NF-κB, nuclear factor-κB; MAPK, Mitogen-Activated Protein Kinase; ERK, extracellular signal regulated kinase; JNK, c-Jun NH2-terminal protein kinase; Akt, protein kinase B; HO-1, hemeoxygenase-1; Nrf2, Nuclear factor erythroid 2-related factor 2.

Declarations

Ethics approval and consent to participate

Not applicable.

Consent for publication

Not applicable.

Availability of data and materials

The datasets generated during the current study are available in the [NCBI] repository, [GenBank accession number: OM919543. SRA accession number: PRJNA814082].

Competing interests

The authors declare no conflict of interest.

Authors' contributions

Conceptualization, Yang-yang Yu; methodology, Yang-yang Yu.; validation, Yang-yang Yu, Si-man Zheng, Ran Fang; writing-original draft preparation, Si-man Zheng; writing—review and editing, Si-man Zheng, Yang-yang Yu; supervision, Ying Xu. All authors have read and agreed to the published version of the manuscript.

References

1. Cekici A , Kantarci A , Hasturk H , et al. Inflammatory and immune pathways in the pathogenesis of periodontal disease[J]. Periodontology 2000, 2014, 64(1): 57-80.
2. Ahn C B , Jung W K , Park S J , et al. Gallic acid-g-chitosan modulates inflammatory responses in LPS-stimulated RAW264.7 cells via NF-κB, AP-1, and MAPK pathways[J]. Inflammation, 2016. 39(1): 366-374.
3. Fujiwara N , Kobayashi K . Macrophages in Inflammation[J]. Current Drug Targets - Inflammation & Allergy, 2005, 4(3): 281-6.
4. Jou I M , Lin C F , Tsai K J , et al. Macrophage-mediated inflammatory disorders[J]. Mediators of Inflammation, 2013, 2013(1): 316482.
5. Rossol M , Heine H , Meusch U , et al. LPS-induced cytokine production in human monocytes and macrophages[J]. Critical Reviews in Immunology, 2011, 31(5): 379.
6. Konrad F M , Knausberg U , Hoene R , et al. Tissue heme oxygenase-1 exerts anti-inflammatory effects on LPS-induced pulmonary inflammation[J]. Mucosal Immunology, 2016, 9(1): 98-111.
7. Jianhua , Rao , Ling , et al. ATF3-mediated NRF2/HO1 signaling regulates TLR4 innate immune responses in mouse liver ischemia/reperfusion injury[J]. American Journal of Transplantation, 2015, 15(1): 76-87.
8. Jin M, Park SY, Shen Q, Lai Y, Ou X, Mao Z, Lin D, Yu Y, Zhang W. Anti-neuroinflammatory effect of curcumin on Pam3CSK4-stimulated microglial cells[J]. Int J Mol Med, 2018, 41(1): 521-530.

9. Newman D J , Cragg G M . Natural products as sources of new drugs from 1981 to 2014[J]. Journal of Natural Products, 2016, 79(3): 629-661.

10. Manita K , Periyasamy S , Deng Z , et al. Deep sea actinomycetes and their secondary metabolites[J]. Frontiers in Microbiology, 2017, 1(8): 760.

11. Pathom-Aree W , Stach J , Ward A C , et al. Diversity of actinomycetes isolated from challenger deep sediment (10,898 m) from the Mariana Trench[J]. Extremophiles, 2006, 10(3): 181-189.

12. Murray P J , Wynn T A . Protective and pathogenic functions of macrophage subsets[J]. Nature Reviews Immunology, 2011, 11(11): 723-37.

13. Laskin , DL , Sunil , et al. Macrophages and tissue injury: agents of defense or destruction[J]. Annual Review of Pharmacology and Toxicology, 2011, 2011, 51: 267-288.

14. Dickhout J G , Basseri S , Austin R C . Macrophage function and its impact on atherosclerotic lesion composition, progression, and stability: the good, the bad, and the ugly[J]. Arteriosclerosis, thrombosis, and vascular biology, 2008, 28(8):1413-1415.

15. Xia Q , Hu Q . Wang H , et al. Induction of COX-2-PGE2 synthesis by activation of the MAPK/ERK pathway contributes to neuronal death triggered by TDP-43-depleted microglia[J]. Cell Death & Disease, 2015, 6(3): e1702.

16. Murakami A , Ohigashi H . Targeting NOX, INOS and COX-2 in inflammatory cells: chemoprevention using food phytochemicals[J]. International Journal of Cancer, 2010, 121(11): 2357-2363.

17. Zhang JM, An JX. Cytokines, inflammation and pain[J]. International Anesthesiology Clinics, 2007, 45(2):27-37.

18. Pan M H , Lai C S , Ho C T . Anti-inflammatory activity of natural dietary flavonoids[J]. Food & Function, 2010, 1(1): 15.

19. Dinarello, Charles A . Overview of the IL-1 family in innate inflammation and acquired immunity[J]. Immunological Reviews, 2018, 281(1): 8-27.

20. Brasier A R . The nuclear factor- B-interleukin-6 signalling pathway mediating vascular inflammation[J]. Cardiovascular Research, 2010, 86(2): 211-218.

21. Arthur J , Ley S C . Mitogen-activated protein kinases in innate immunity[J]. Nature Reviews Immunology, 2013, 13(9): 679-692.

22. Kane L P , Mollenauer M N , Xu Z , et al. Akt-dependent phosphorylation specifically regulates cot induction of NF-κB-dependent transcription[J]. Molecular & Cellular Biology, 2002, 22(16): 5962.

23. Kenneth , D , Poss, et al. Reduced stress defense in heme oxygenase 1-deficient cells[J]. Proceedings of the National Academy of Sciences of the United States of America, 1997, 94(20): 10925-30.

24. P Fernández, MI Guillén, F Gomar, et al. Expression of heme oxygenase-1 and regulation by cytokines in human osteoarthritic chondrocytes[J]. Biochemical Pharmacology, 2003, 66(10): 2049-2052.

25. Yeh P Y , Li C Y , Hsieh C W , et al. CO-releasing molecules and increased heme oxygenase-1 induce protein S-glutathionylation to modulate NF-κB activity in endothelial cells[J]. Free Radical Biology & Medicine, 2014, 70: 1-13.

26. Vaeth M , Feske S . NFAT control of immune function: new frontiers for an abiding trooper[J]. F1000Research, 2018, 7: 260.

27. Guha M , Mackman N . LPS induction of gene expression in human monocytes[J]. Cellular Signalling, 2001, 13(2): 85-94.
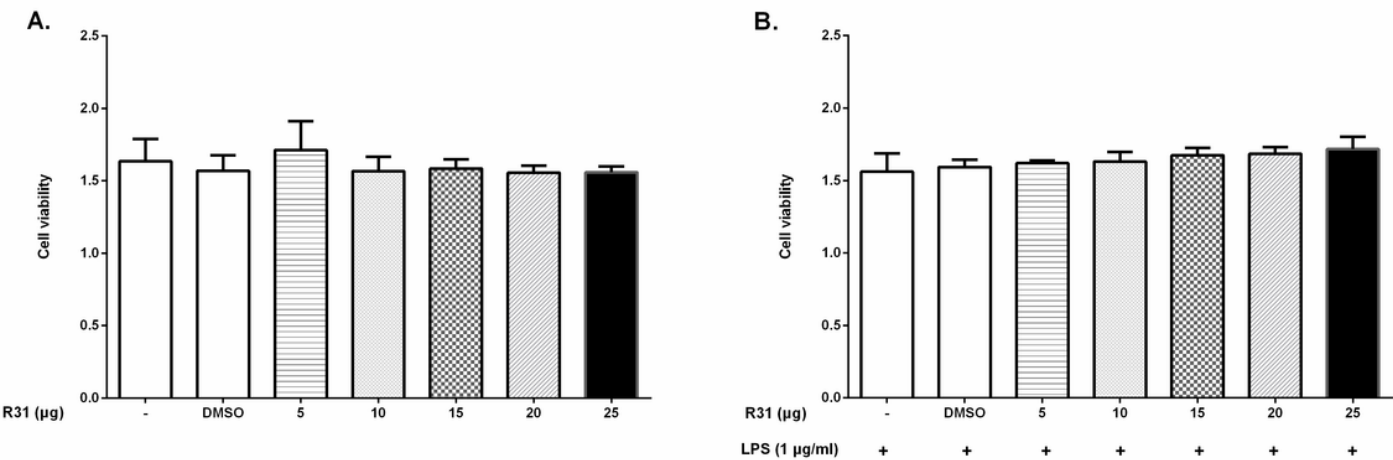
Figures

Figure 1

Effect of R31 crude extract on RAW264.7 macrophage cell viability. (A) RAW264.7 cells were treated with various concentrations of R31 crude extract (5, 10, 15, 20 and 25 µg/ml) for 24 h. (B) RAW264.7 cells were pretreated with R31 crude extract (5, 10, 15, 20 and 25 µg/ml) for 1 h, and followed by LPS (1 µg/ml) for 24 h. Cell viability was measured by CCK-8 assay. Statistical significance were expressed ±S.D. for three independent experiments (n = 3).
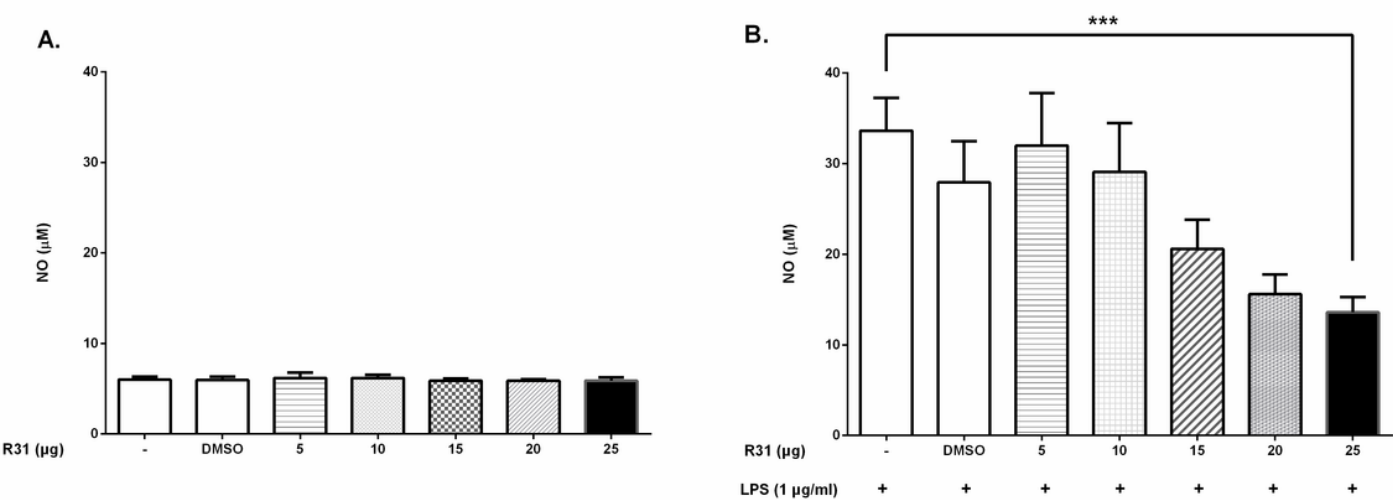
Figure 2

Effect of R31 crude extract on LPS-induced NO expression in RAW264.7 macrophage cell. Cells were pretreated with R31 crude extract at increasing doses (0-25 μg/ml) and stimulated with LPS (1 μg/ml). NO levels were measured using the Griess reagent after 24 h of LPS-induced. Data were presented as the mean (SD) of triplicate experiments. ∗P < 0.05, ∗∗P < 0.01 vs. the LPS-treated control.
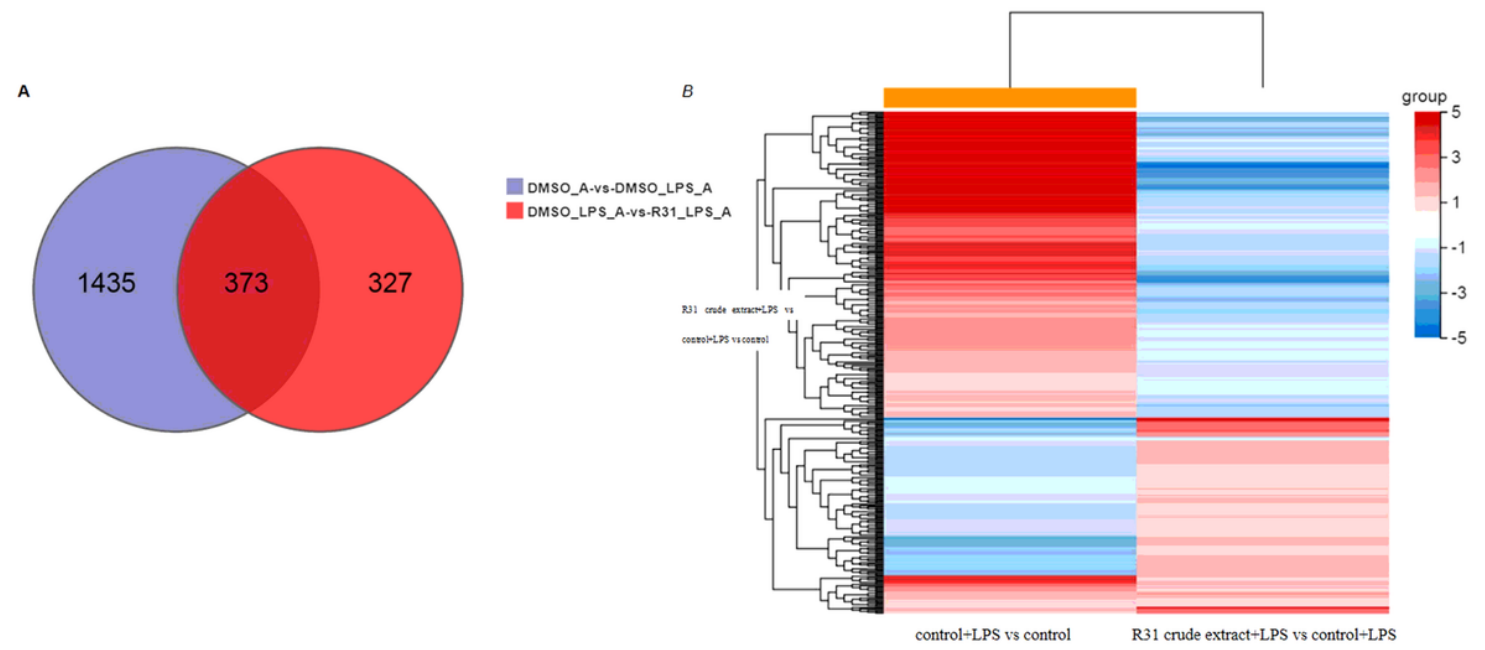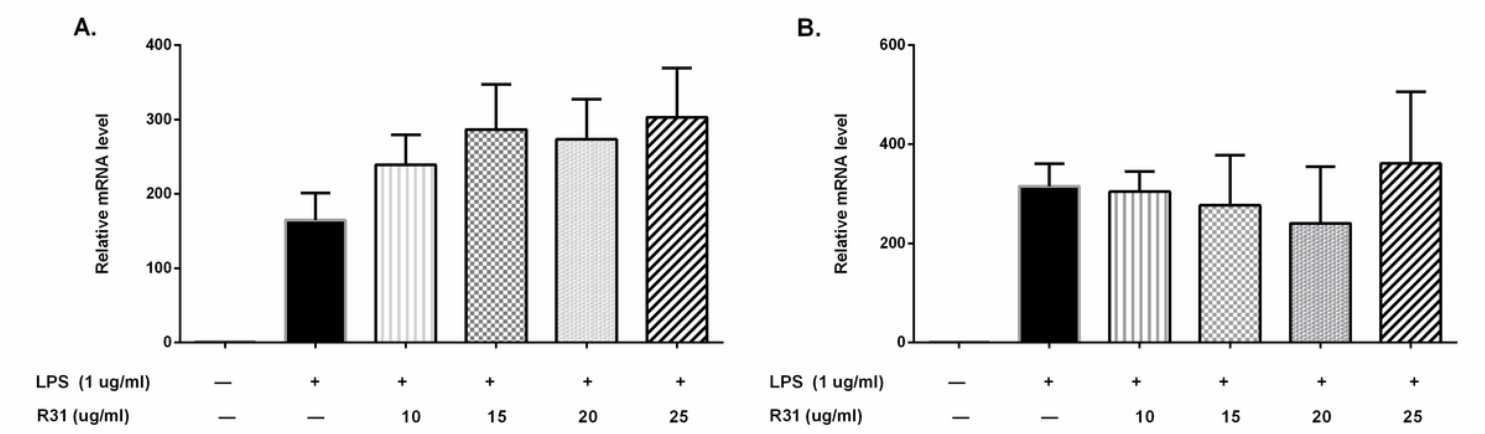

Figure 3

DEGs profiling by RNA-sequence related to R31 crude extract in LPS-stimulated RAW 264.7 cells. (A) Venn diagram with DEGs related to control+LPS vs control group and R31 crude extract+LPS vs control+LPS group. (B) Heat map representing DEGs up-regulated or reduced between two groups.
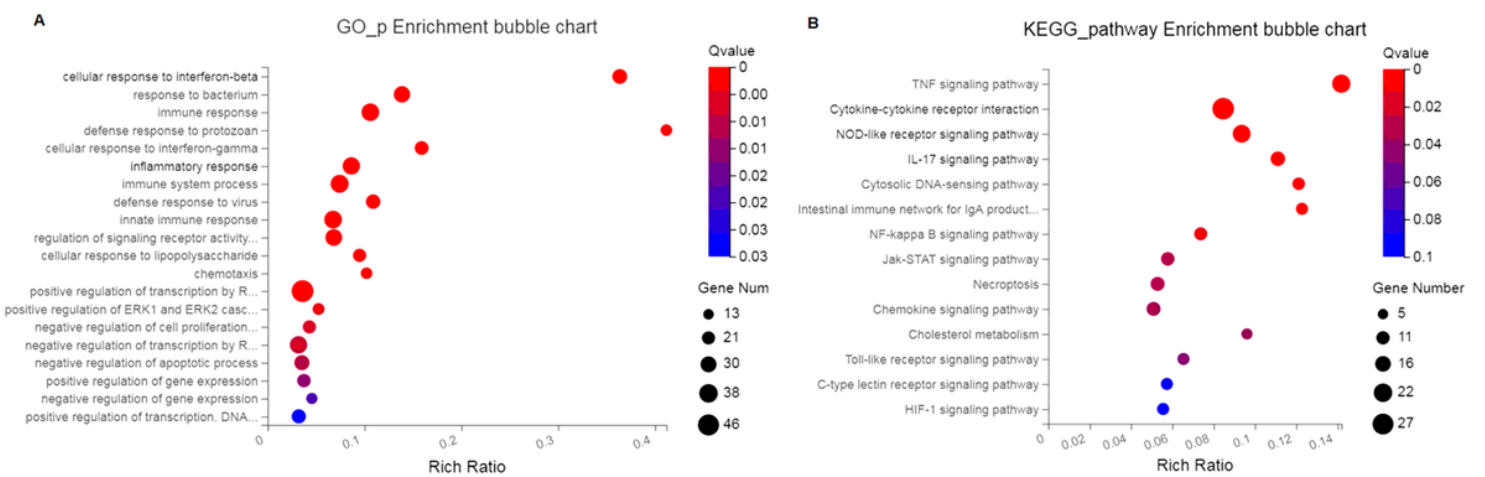
Figure 4

Function analysis of DEGs by GO & KEGG. (A) GO terms on Biological Process of DEGs. The vertical axis represents the Biological Process. The horizontal axis represents the enrich factor. The top 20 Go terms were selected according to the gene number. Different colors from red to blue represent p-value, and the size of the dot represents the gene count number. (B) KEGG pathway functional enrichment analyses of co-expressed DEGs in control+LPS vs control group and R31 crude extract+LPS vs control+LPS group.

Figure 5

Effect of R31 crude extract on LPS-induced COX-2, iNOS expression in RAW264.7 macrophage cell. Cells were pretreated with R31 crude extract at increasing doses (0-25 µg/ml) and stimulated with LPS (1 µg/ml). The mRNA expression levels of (A) COX-2 and (B) iNOS were detected using RT-qPCR analysis after 4 h of LPS-induced. Data were presented as the mean (SD) of triplicate experiments. *P < 0.05, **P < 0.01 vs. the LPS-treated control.
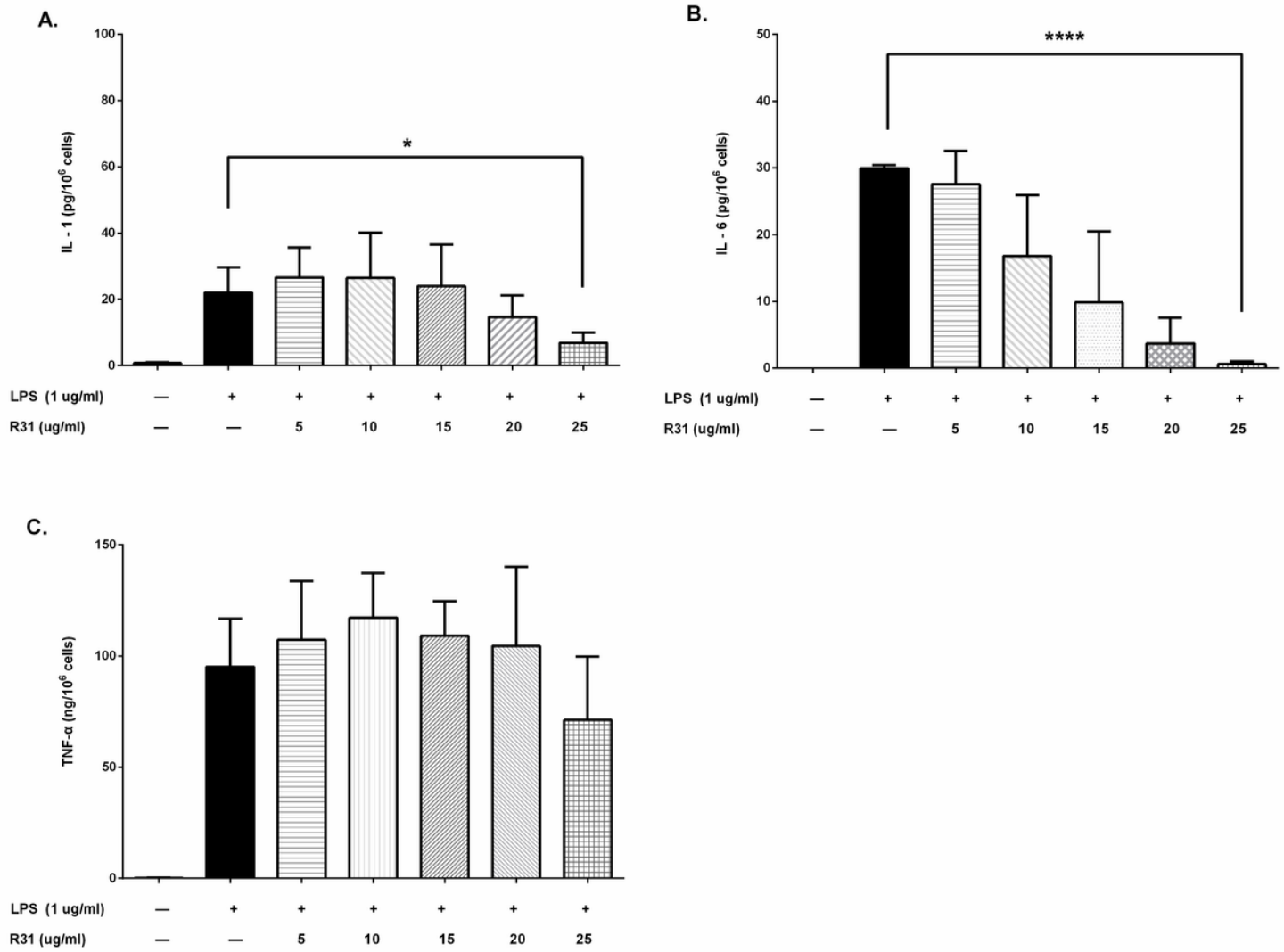
Figure 6

Effect of R31 on the release of IL-1, IL-6, TNF-α in RAW264.7 macrophage cell. Cells were pretreated with R31 at increasing doses (0-25 μg/ml) and stimulated with LPS (1 μg/ml) for 24 h. The secretion of (A) IL-1, (B) IL-6, (C) TNF-α were determined by ELISA. Values were expressed the mean ±S.D. for three independent experiments. ∗P < 0.05, ∗∗P < 0.01 vs. the LPS-treated control.
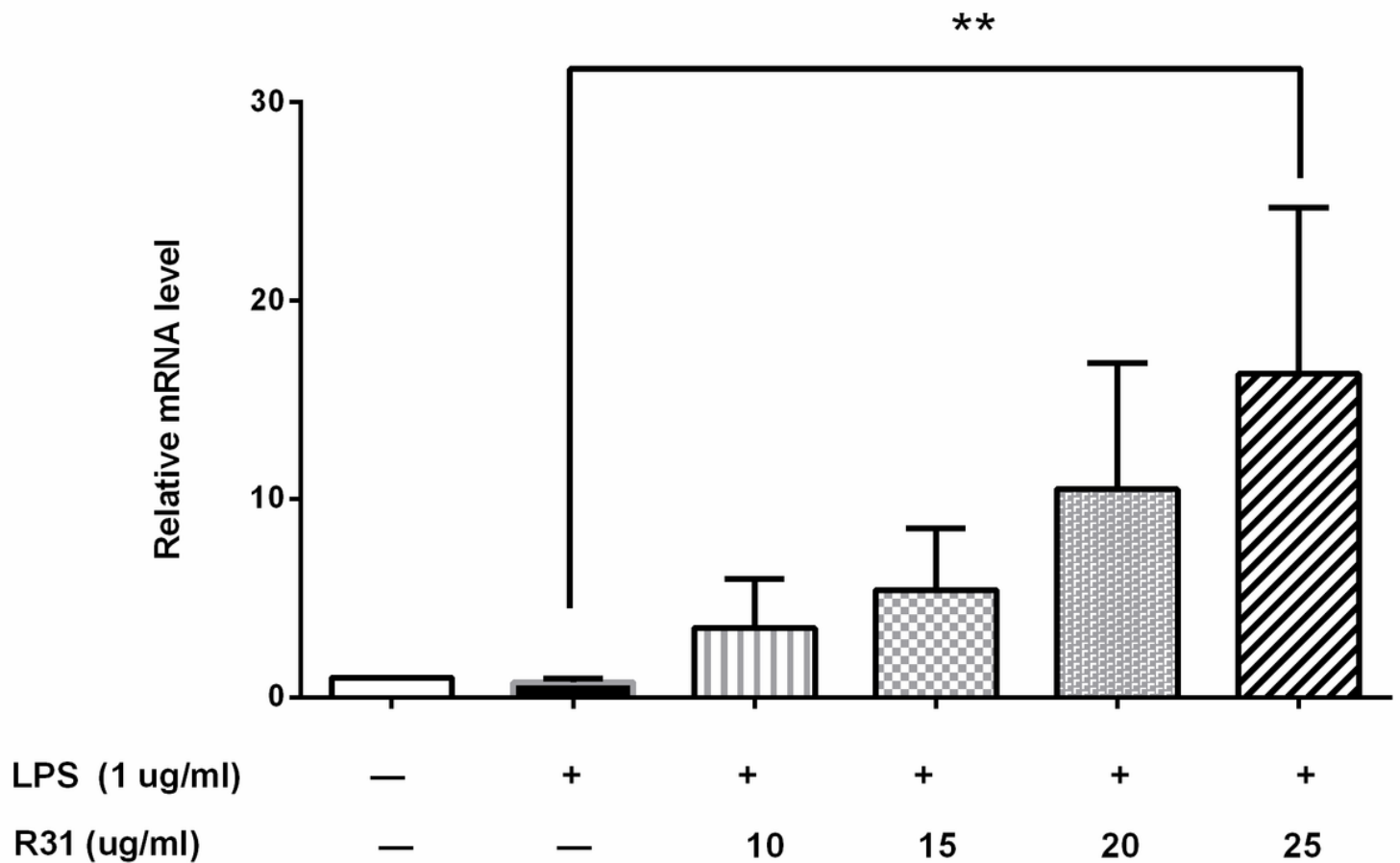
Figure 7

Effect of HO-1 on R31 crude extract-mediated anti-inflammatory effects in LPS-induced RAW264.7 macrophage cell. Cells were incubated with R31 crude extract at increasing concentrations (0-25 μg/ml) for 4 h. The mRNA expression level of HO-1 was detected by RT-qPCR. The results were presented as the mean ±SD of triplicate experiments. *p<0.05, **p<0.01, and ***p<0.001 versus negative control.
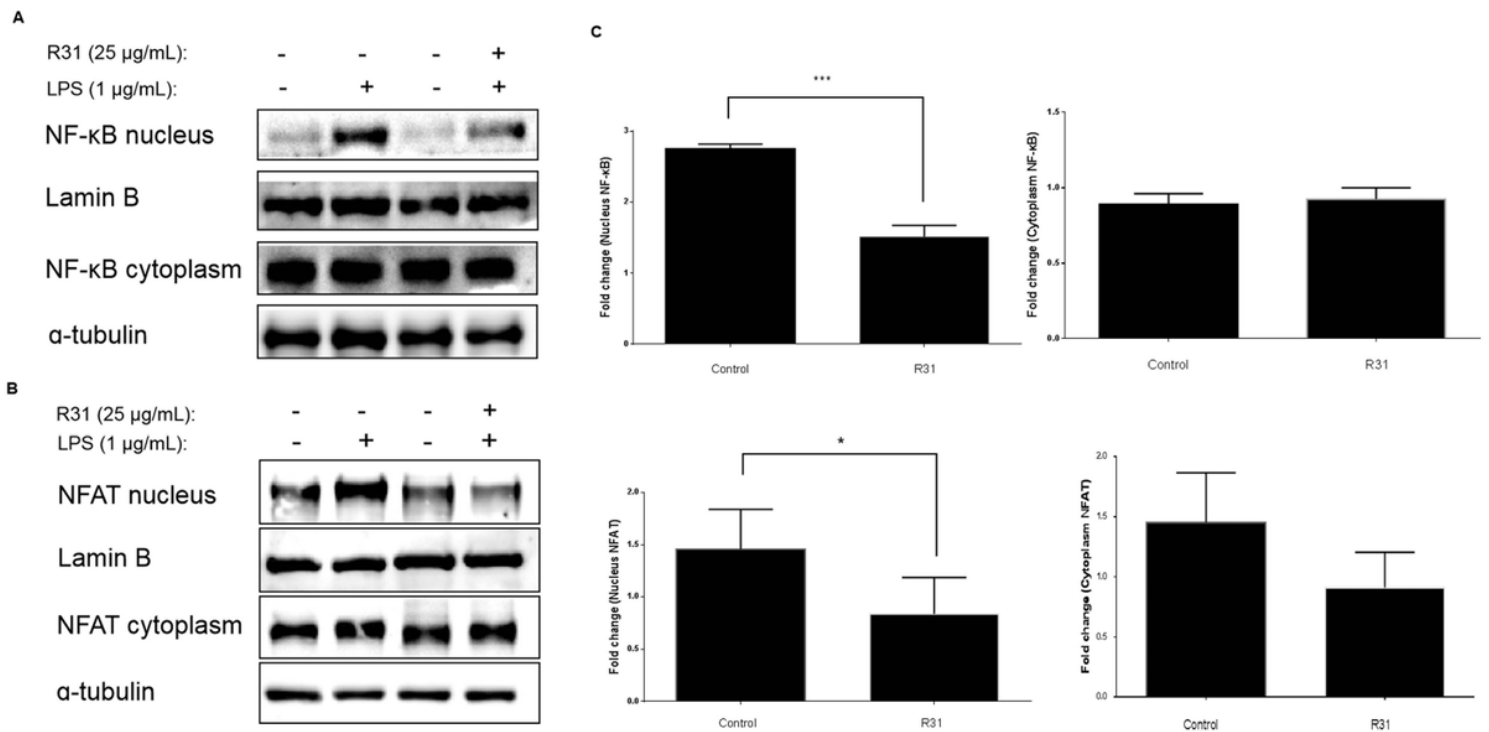
Figure 8

Effects of R31 crude extract on NF-κB and NFAT1 activation in LPS-induced RAW264.7 macrophage cells. Cells were pretreated with R31 crude extract at 25 μg/ml for 1 h before 30 min of LPS (1 μg/ml) stimulaion. The degree of NF-κB and NFAT1 in the Nucleus and cytoplasm were confirmed by Western blot. Lamin B1 and α-tubulin were used as a protein-loading control in the nucleus and cytoplasm respectively (A and B). (C) Relative level of protein expression between control and R31 crude extract were compared.
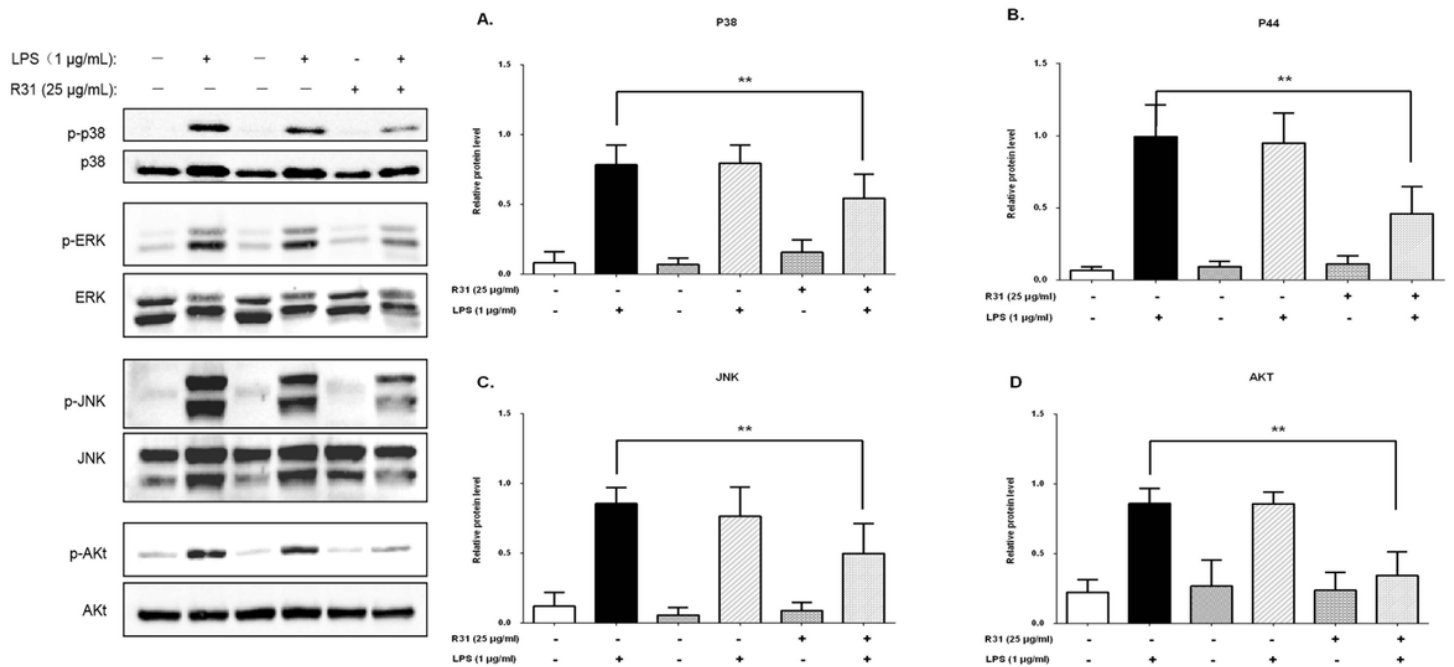
Figure 9

Effect of R31 crude extract on LPS-induced phosphorylation of p38, ERK1/2, JNK and Akt in RAW264.7 macrophage cell. Cells were pretreated with R31 crude extract (25 µg/ml) for 1 h and then stimulated with LPS (1 µg/ml) for 15 min. Equal amount of cell extracts were collected and assessed by Western blot. Total p38, ERK1/2, JNK and Akt were used as internal controls. The grouping of blots were blotting in the same gel (phosphorylation vs total protein) and the relative protein levels (A, B, C and D) were determined. Each bar represents the mean ± standard deviation from triplicate experiments. *$p<0.05$, **$p<0.01$, and ***$p<0.001$ compared to the LPS group.